Commun. Comput. Chem.
doi: 10.4208/cicc.2015.v3.n2.3

Vol.**3**, No.**2**, pp.55-65
September 2015

REGULAR ARTICLE

A DFT/TDDFT Investigation on Intramolecular Proton Transfer of Bis(imino)isoindole

Chi Ma, Hongsheng Zhai, Yonggang Yang, Yufang Liu*

College of Physics and Electronic Engineering, Henan Normal University, Xinxiang 453007, China

Received 20 July 2015; Accepted (in revised version) 10 September 2015

Abstract: The density functional theory (DFT) and time-dependent density functional theory (TDDFT) method were carried out to investigate intramolecular hydrogen bond and intramolecular proton transfer of Bis(imino)isoindole in the ground- and excited-state. From the analysis of IR spectra, electronic spectra and the corresponding frontier molecular orbitals, we found that the intramolecular hydrogen bond I is strengthened while the intramolecular hydrogen bond II is weakened in BII molecule in the S1 state. The potential energy curve shows that the proton cannot spontaneously transferred in the ground state because of the relative high potential energy barrier. After photo-excitation, the strengthening of intramolecular hydrogen bond I may lower the potential energy barrier and then promote the proton transfer.

AMS subject classifications: 74E40, 78M50

Keywords: ESIPT, Spectral properties, Potential Energy curve, Excited-state hydrogen bond

1 Introduction

The photo-induced excited-state proton transfer (ESPT) has been extensively studied due to its important role in physical and biological systems. Weller and co-workers [1] firstly observed the excited-state proton transfer phenomenon of methyl salicylate in the characteristic experiment. Taylor and co-workers [2] found that the 7-azaindole dimer has different tautomer in ground and first excited states. Sengupta et al. [3] were used proton

---

* Corresponding author *E-mail address*: yf-liu@htu.cn (Y. F. Liu)

transfer theory to explained the dual fluorescence in 3-hydroxyflavone. Chou and co-workers [4] described a functioning photo-induced proton transfer of 3-hydroxyflavone in the excited-state occurs in less than 8ps. The hydrogen bond is found to be very important in excited-state proton transfer process [5-9] for its good directional character. Recently, Han and co-workers have presented a new mechanism that the intermolecular hydrogen bond is significantly strengthened upon photo-excitation [10-14]. On the basis of the great success of hydrogen bond strengthened theory, many phenomena such as excited-state hydrogen bond dynamic and proton transfer (PT) reaction should be revisited.

The spectroscopic techniques can only give indirect information about the excited-state intramolecular proton transfer, so there are still some unsolved problem about the specific role of intra- and intermolecular hydrogen-bond interactions in the ESPT process. And the wide use and reliable accuracy of the density functional theory (DFT) and time-dependent density functional theory (TD-DFT) give us a new way to study the excited state proton transfer. In the present work, the Bis(imino)isoindole (BII) and its isomer are optimized in the ground and excited states using the DFT and TDDFT methods at B3LYP/6-31++g(d) level based on CPCM model in methanol. The configurations of the molecules are shown in the Figure1. The IR spectral shifts of O-H and N-H vibrational modes in the molecules are monitored to predict the changes of intramolecular hydrogen bond. Moreover, the electronic spectra, frontier molecular orbitals and potential energy curves are also calculated to investigate the intramolecular proton transfer mechanisms.

2 Computational details

All the computations were performed using the Gaussian09 program package[15] at the popular Becke's three-paremeter hybrid exchange functional with Lee–Yang–Parr gradient-corrected correlation (B3LYP) [16] with the standard 6-31++G(d) level. The 6-31++G(d) basis set has sufficient flexibility to describe the system and chosen as the basis set throughout. The geometric optimizations were performed by DFT method in the S_0 state and TDDFT method in the S_1 state. The TD-DFT method has been proved to be very useful to describe the hydrogen bond system in the excited states. The methanol was selected as the solvent in the calculations and the continuum polarizable continuum model (CPCM) [17, 18] was chosen to evaluate solvent effects. These computations were performed on BII and its isomer without any constraint of bonds, angles, dihedral angles or symmetry. All the local minima geometries are confirmed by the absence of an imaginary mode in vibrational analysis and calculations.

3 Results and discussion

3.1 The optimized geometric structures and infrared spectra

The geometry optimizations of BII in the ground and excited states were performed by destiny functional theory (DFT) and time-dependent destiny functional theory (TD-DFT) methods at B3LYP/6-31++g(d) level in methanol based on CPCM. All the local minima both in the S_0 and S_1 states have the real frequencies. The configuration of BII and its isomer with their corresponding molecular electrostatic potential (MEP) maps are presented in **Figure 1**. Some of the most primary structural parameters are chosen to list in the **Table 1**. From **Table 1,** it is shown clearly that the O-H bond length was lengthened from 0.9858Å (S_0) to 0.9916Å (S_1). Meanwhile, the N-H bond length is shortened from 1.0252Å (S_0) to 1.0233Å (S_1). It also should be noted that the bond angle $\delta_{(O\text{-}H\cdots N)II}$ changes from 142.42° to 145.06° after photo-excitation, which is much closer to 180°. While the bond angle $\delta_{(O\cdots H\text{-}N)I}$ changes from 133.97° to 132.64°after photo-excitation. According to above evidence, it is easy to conclude that the intramolecular hydrogen bond II is strengthened while intramolecular hydrogen bond I is weakened after photo-excitation. The N-H bond lengths are both change from 1.0195Å in the S_0 state to 1.0233Å in the S_1 state in the keto-BII, which indicate that the intramolecular hydrogen bonds are both slightly strengthened after photo-excitation.

Table 1 Calculated bond lengths (Å) and angles (°) of Bis(imino)isoindole and its isomer in the S_0 and S_1 states.

BII	O-H	N-H	$\delta_{(O\cdots H\text{-}N)I}$	$\delta_{(O\text{-}H\cdots N)II}$
S_0	0.9858	1.0252	133.97	142.42
S_1	0.9916	1.0233	132.64	145.06
Keto-BII	$(N\text{-}H)_I$	$(N\text{-}H)_{II}$	$\delta_{(O\cdots H\text{-}N)I}$	$\delta_{(O\cdots H\text{-}N)II}$
S_0	1.0195	1.0195	129.69	129.69
S_1	1.0223	1.0223	131.01	131.01

The vibrational modes of functional groups involved in the hydrogen bonds are closely related to the hydrogen-bond strengthening and weakening [19,20]. So the calculated O-H and N-H stretching vibration spectra of BII molecule both in the S_0 and S_1 states are shown in **Figure2 (a).** It can be seen that the O-H stretching vibrational frequency are located at 3472cm^{-1} in the S_0 state and 3361cm^{-1} in the S_1 state. A strong redshift about 111cm^{-1} happened due to the intramolecular hydrogen bond strengthening after photo-excitation. Furthermore, the N-H stretching vibrational frequencies are located at 3406cm^{-1} in the S_0

state and 3439cm^{-1} in the S_1 state. A slight blueshift about 33cm^{-1} happened due to the intramolecular hydrogen bond weakening after photo-excitation. From **Figure2(b)**, it also can be noted that the two N-H stretching vibrational frequency are located at 3502cm^{-1} in the S_0 state and 3458cm^{-1} in the S_1 state. A slight redshift about 44cm^{-1} happened due to the intramolecular hydrogen bond strengthening after photo-excitation. The vibration spectra analyses are in good agreement with the bond and angle analysis above.

The ESP maps are based on the conventional color spectrum. The potential increases from red to blue, which goes by an order of red < orange < yellow < green < blue. As is shown in **Figure1,** for the molecule BII, the region of oxygen atom of intramolecular hydrogen bond (O···H-N) is entirely red, which means there are mainly the negative electrostatic potential located around the oxygen atom. In the intramolecular hydrogen bond (O-H···N), the negative electrostatic potential located on oxygen atom is much less. Two different kinds of intramolecular hydrogen bonds exist in the same molecule; the potential distribution shows difference clearly. Meanwhile, in the molecule keto-BII, the negative electrostatic potential are mainly located on oxygen atom in the intramolecular hydrogen bond (O···H-N). It may indicate that the intramolecular hydrogen bond influence the potential distribution in the molecule.

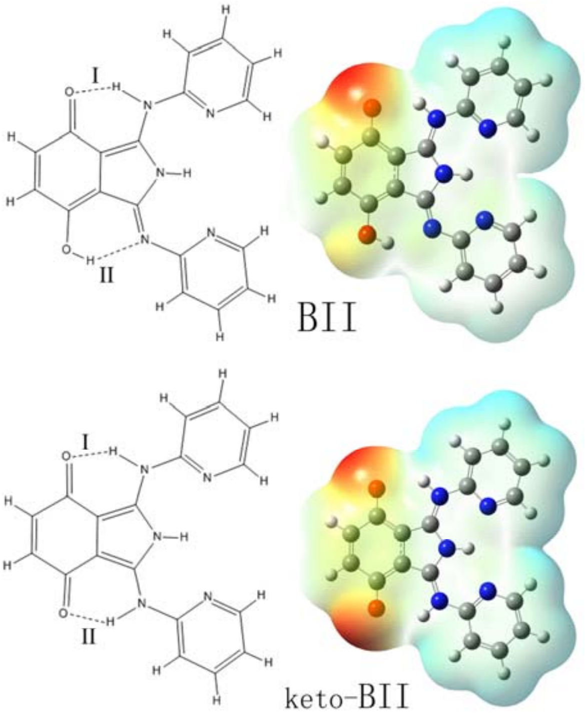

Figure 1: The configuration of Bis(imino)isoindole and its isomer with their corresponding molecular electrostatic potential (MEP) map.

3.2 Electronic spectra and frontier molecular orbitals

Based on the TDDFT/B3LYP/6-31++g(d) calculated level, the corresponding absorption and emission spectra of BII are displayed in **Figure 3**. The calculated absorption spectrum of BII is located at 540nm. The lowest excited state of BII and keto-BII molecules are fully optimized by TDDFT method based on the ground state optimized geometric conformations. The emission spectrum of BII is at 648nm while that of the keto-BII is at 676nm. The red-shift about 28nm may due to the intramolecular proton transfer and the changes of different kinds of intramolecular hydrogen bonds.

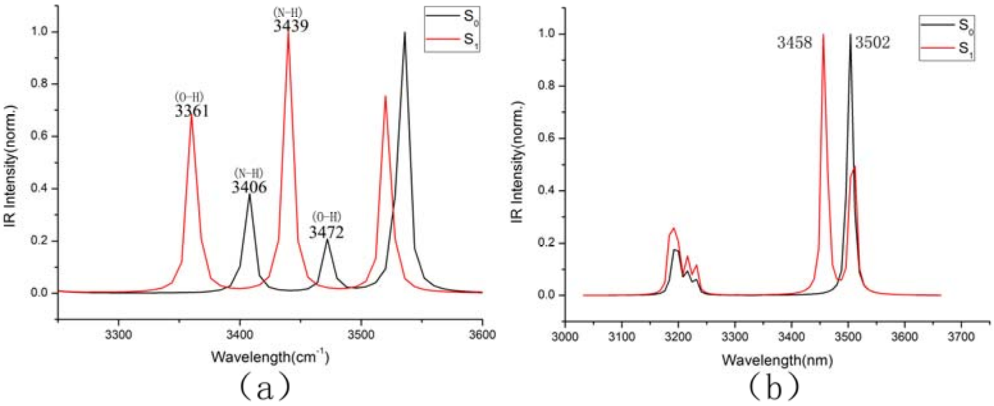

Figure 2: The calculated stretching vibration spectra in the S_0 and S_1 states, (a) the O-H and N-H in Bis(imino)isoindole, (b) the N-H in its isomer.

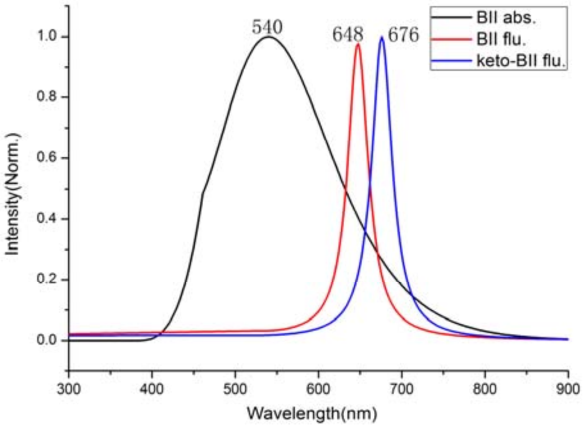

Figure 3: The absorption spectum and emission spectra of Bis(imino)isoindole and its isomer at B3LYP/6-31++g(d) level.

The charge redistribution are closed related to the change of hydrogen bond, so the Mulliken charge distribution also been presented in **Figure 4** and discussed in detail. For the intramolecular hydrogen bond (O···H-N) in BII, the charge of atom O_1 is calculated to be -0.7333 in the ground state and changes to -0.6628 in the S_1 state, the charge of atom H_{13} decreases about 0.0055 from 0.5888 in the S_0 state to 0.5833 in the S_1 state. Compared with that in the ground state, the charge of nitrogen atom is less negative in the S_1 state, which implies that the intramolecular hydrogen bond (O···H-N) is weakened in the S_1 state. In the intramolecular hydrogen bond (O-H···N), the charge of atom N_4 is calculated to be -0.4885 in the ground state and changes to -0.4814 in the S_1 state, the charge of atom H_1 changes from 0.5973 in the S_0 state to 0.6059 in the S_1 state.

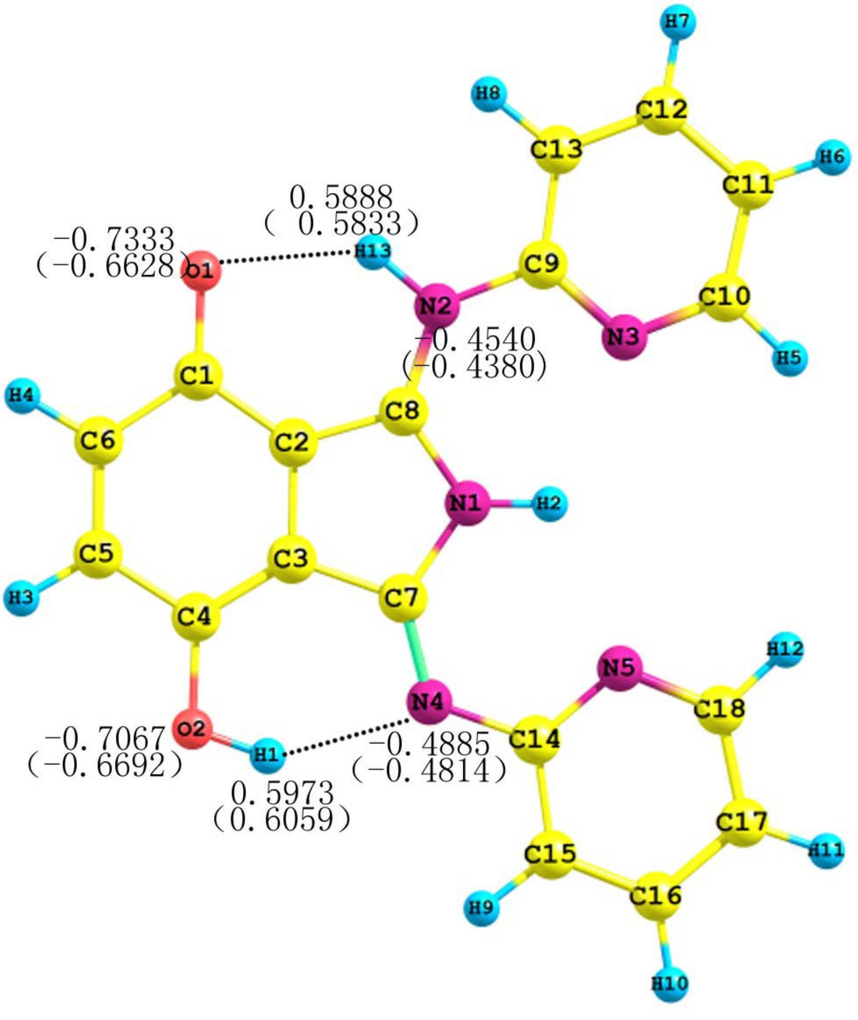

Figure 4: The Mulliken charges of labeled atoms in ground state and excited state (in parenthesis).

The frontier molecular orbitals (FMOs) can reflect the molecular properties in the excited states well, and the S_1 state of BII is primarily contributed by the orbital transition from the HOMO to the LUMO (97.9%). Therefore, only the HOMO and LUMO orbitals of BII are discussed in detail and shown in **Figure5**. The frontier molecular orbitals of the keto-BII molecule are set for comparison. And the intense transition from the S_0 state to the S_1 state for BII is at 540nm with the oscillator strength of 0.4525. It is easy to note that the π character for the HOMO and the π^* character for LUMO, so the transition is a predominant $\pi\pi^*$-type transition from the highest occupied molecular orbital (HOMO) to the lowest unoccupied molecular orbital (LUMO). The change of electron density in the hydrogen bond donor and acceptor groups can directly influences the intramolecular hydrogen bonds. In addition, the charge transfer is primarily from the O atom to the N atom along with the intramolecular hydrogen bond upon excitation. The electron density located on the oxygen atom decreases from HOMO to LUMO, and the density located on the nitrogen atom increases. The charge transfer along with the O-H···N may directly strengthen the intramolecular hydrogen bond, but the transfer along with the O···H-N weaken the intramolecular hydrogen bond inversely. In the molecule keto-BII, the electron density located on the oxygen atoms has little change after photo-excitation, but decrease clearly on the H-N groups. It may indicate that the intramolecular hydrogen bonds are both strengthened in the S_1 state.

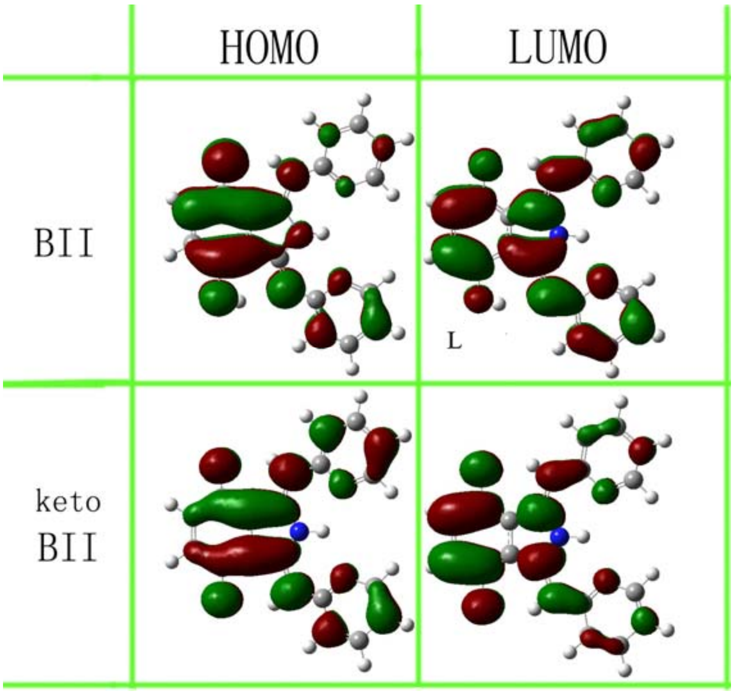

Figure 5: Frontier molecular orbitals (HOMO and LUMO) of Bis(imino)isoindole its isomer.

3.3 Potential energy curves

In order to reveal the excited state intramolecular proton transfer mechanism more clearly, the geometrical structures both in the ground state and the first excited state were optimized with fixed O-H bond length at TD-DFT/B3LYP/6-31++g(d) with the CPCM solvation model for methanol. The potential energy curves with construction though varying the O-H bond lengths from 0.98 to 2.18 Å in steps of 0.1 Å and shown in **Figure 6**. In spite of the TD-DFT/B3LYP method has not been proved sufficiently accurate to describe the excited states, but the previous calculations indicated that the method is reliable enough investigate the intermolecular proton transfer process. From **Figure 6**, it is easy to note that the energy of BII in the S_0 state decreases about 2.742kcal/mol after a potential barrier about 9.35 kcal/mol with the increase of O-H bond length. And the energy in the S_1 state decreases about 3.069kcal/mol along with the increase of the hydroxyl bond length, there is only a low potential barrier about 7.32kcal/mol. Therefore, the single intramolecular proton transfer may not spontaneous occur in the S_0 state, but the ESIPT is probably happen duo to the decrease of energy and low energy barrier in the S_1 state. As discussed above, the intramolecular hydrogen bond I is strengthened in the S_1 state, which means the hydrogen bond strengthen may lower the energy barrier and promote the transition of proton. Moreover, the calculated energy curve is in corresponding with the radiative transition process, and their florescence emission peaks are located at 648nm and 676nm, respectively.

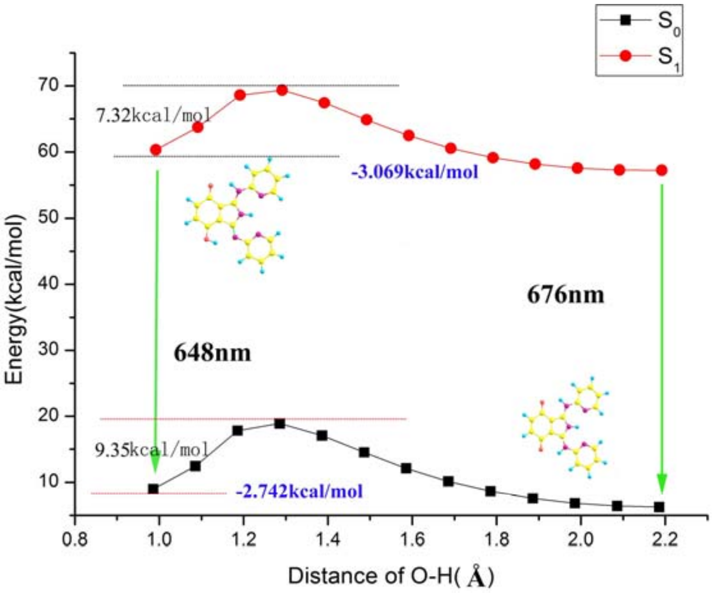

Figure 6: Potential energy curves of the S_0 and S_1 states for Bis(imino)isoindole molecule along with O–H bond length.

4 Conclusion

In this work, the ground and excited states hydrogen bonding dynamics and excited-state intramolecular proton transfer of Bis(imino)isoindole are theoretically investigated by DFT and TDDFT methods. It is found that intramolecular hydrogen bond I is strengthened while the intramolecular hydrogen bond II is weakened after photo-excitation. The frontier molecular orbitals and the Mulliken charge distribution are also present to investigate the proton transfer mechanism. It is easy to note that the charge transfer is mainly from the oxygen atom to the nitrogen atom along with the intramolecular hydrogen bond upon excitation. Therefore, we may indicate that the charge redistribution can directly influence the intramolecular proton transfer. Moreover, the potential energy curves of the ground and first excited states are scanned through varying the O–H bond length. The strengthening of intramolecular hydrogen bond may lower the potential energy barrier in the S_1 state and then promote the proton transfer.

Acknowledgements

This work is supported by National Natural science Foundation of China (Grant no. 11274096), Innovation Scientists and Technicians Troop Construction Projects of Henan Province (Grant no. 124200510013) and Supported by Program for Innovative Research Team (in Science and Technology) in University of Henan Province (Grant no. 13IRTSTHN016).

Reference

[1] H. Beens, K. Grellmann, M. Gurr, A. Weller, Effect of solvent and temperature on proton transfer reactions of excited molecules, Dis. Fara. Soc., 39 (1965), 183-193.

[2] B. Dellinger, M. Kasha, Phenomenology of solvent matrix spectroscopic effects, Chem. Phys. Lett., 38 (1976), 9-14.

[3] P.K. Sengupta, M. Kasha, Excited state proton-transfer spectroscopy of 3-hytdroxyflavone and quercetin, Chem. Phys. Lett., 68 (1979), 382-385.

[4] D. McMorrow, T.P. Dzugan, T.J. Aartsma, Excited-state dynamics of the intramolecular proton transfer of 3-hydroxyflavone in the absence of external hydrogen-bonding interactions, Chem. Phys. Lett., 103 (1984), 492-496.

[5] A.L. Sobolewski, W. Domcke, C. Hättig, Tautomeric selectivity of the excited-state lifetime of guanine/cytosine base pairs: The role of electron-driven proton-transfer processes, P Natl. Acad. Sci. USA, 102 (2005), 17903-17906.

[6] K. Das, N. Sarkar, A.K. Ghosh, D. Majumdar, D.N. Nath, K. Bhattacharyya, Excited-state intramolecular proton transfer in 2-(2-hydroxyphenyl) benzimidazole and-benzoxazole: effect of

rotamerism and hydrogen bonding, J Phys. Chem., 98 (1994), 9126-9132.

[7] T. Elsaesser, H. Van den Akker, Ultrafast hydrogen bonding dynamics and proton transfer processes in the condensed phase, Springer Science & Business Media, 2013.

[8] L.M. Tolbert, K.M. Solntsev, Excited-state proton transfer: from constrained systems to "super" photoacids to superfast proton transfer, Accounts Chem. Res., 35 (2002), 19-27.

[9] D. McMorrow, M. Kasha, Intramolecular excited-state proton transfer in 3-hydroxyflavone. Hydrogen-bonding solvent perturbations, J Phys. Chem., 88 (1984), 2235-2243.

[10] G.J. Zhao, K.L. Han, Time-dependent density functional theory study on hydrogen-bonded intramolecular charge-transfer excited state of 4-dimethylamino-benzonitrile in methanol, J Comput. Chem., 29 (2008), 2010-2017.

[11] G.J. Zhao, K.L. Han, Role of intramolecular and intermolecular hydrogen bonding in both singlet and triplet excited states of aminofluorenones on internal conversion, intersystem crossing, and twisted intramolecular charge transfer, J Phys. Chem. A, 113 (2009), 14329-14335.

[12] G.J. Zhao, K.L. Han, Site-specific solvation of the photoexcited protochlorophyllide a in methanol: formation of the hydrogen-bonded intermediate state induced by hydrogen-bond strengthening, Biophys. J, 94 (2008), 38-46.

[13] G.J. Zhao, R.K. Chen, M.T. Sun, J.Y. Liu, G.Y. Li, Y.L. Gao, K.L. Han, X.C. Yang, L. Sun, Photoinduced intramolecular charge transfer and S2 fluorescence in thiophene-pi-conjugated donor-acceptor systems: experimental and TDDFT studies, Chem. Physi. Chem., 14 (2008), 6935-6947.

[14] D. Pan, X. Cai, C. Yalaz, A. Senpan, K. Omanakuttan, S.A. Wickline, L.V. Wang, G.M. Lanza, Photoacoustic sentinel lymph node imaging with self-assembled copper neodecanoate nanoparticles, ACS nano, 6 (2012), 1260-1267.

[15] M. J. Frisch, G. W. Trucks, H. B. Schlegel, G. E. Scuseria, M. A. Robb, J. R.; Scalmani, G. Cheeseman, V.Barone, B. Mennucci, G. A. Petersson, H. Nakatsuji, M. Caricato, X. Li, H. P. Hratchian, A. F. Izmaylov,J. Bloino, G. Zheng, J. L. Sonnenberg, M. Hada, M. Ehara, K. Toyota, R. Fukuda, J. Hasegawa, M.Ishida, T. Nakajima, Y. Honda, O. Kitao, H. Nakai, T. Vreven, J. A. Montgomery, Jr. J. E. Peralta, F.Ogliaro, M. Bearpark, J. J. Heyd, E. Brothers, K. N. Kudin, V. N. Staroverov, R. Kobayashi, J.Normand, K. Raghavachari, A. Rendell, J. C. Burant, S. S. Iyengar, J. Tomasi, M. Cossi, N. Rega, J. M.Millam, M. Klene, J. E. Knox, J. B. Cross, V. Bakken, C. Adamo, J. Jaramillo, R. Gomperts, R. E.Stratmann, O. Yazyev, A. J. Austin, R. Cammi, C. Pomelli, J. W. Ochterski, R. L. Martin, K. Morokuma,V. G. Zakrzewski, G. A. Voth, P. Salvador, J. Dannenberg, S. Dapprich, A. D. Daniels, O. Farkas, J. B.Foresman, J. V. Ortiz, J. Cioslowski, D. J. Fox, Gaussian 09, Revision A.02; Gaussian, Inc.: Wallingford, CT, 2009.

[16] S. Vosko, L. Wilk, M. Nusair, Accurate spin-dependent electron liquid correlation energies for local spin density calculations: a critical analysis, Can. J Phys., 58 (1980), 1200-1211.

[17] V. Barone, M. Cossi, Quantum calculation of molecular energies and energy gradients in solution by a conductor solvent model, J Phys. Chem. A, 102 (1998), 1995-2001.

[18] M.D. Liptak, G.C. Shields, Accurate p K a calculations for carboxylic acids using complete basis set and Gaussian-n models combined with CPCM continuum solvation methods, J Am. Chem. Soc., 123 (2001), 7314-7319.

[19] H. Li, Y. Yang, D. Yang, Y. Liu, J. Sun, TDDFT study on the excited-state hydrogen bonding of N-(2-hydroxyethyl)-1,8-naphthalimide and N-(3-hydroxyethyl)-1,8-naphthalimide in methanol solution, J Phys. Org. Chem., 27 (2014), 170-176.

[20] H. Li, Y. Liu, Y. Yang, D. Yang, J. Sun, Excited-state intramolecular hydrogen bonding of compounds based on 2-(2-hydroxyphenyl)-1,3-benzoxazole in solution: A TDDFT study, Spectrochim. Acta. A., 133 (2014), 818-824.